Volume 1 • Issue 6 • 2017

Short Communication

Orthopaedic Surgery and Traumatology

ISSN: 2573-4962

Computer Graphic Model of Hydroxyapatite Using Windows

Masayuki Okazaki*

Graduate School of Health Care Science, Jikei Institute, Master Course of Management in Health Care Sciences, Japan

***Corresponding Author:** Masayuki Okazaki, Graduate School of Health Care Science, Jikei Institute, Master Course of Management in Health Care Sciences, 1-2-8 Miyahara, Yodogawa-ku, Osaka 532-0003, Japan.

Received: November 14, 2017; **Published:** November 18, 2017

Abstract

Hydroxyapatite is an inorganic component of bone and teeth. Stoichiometric hydroxyapatite is an ionic crystal with Ca^{2+}, PO_4^{3-}, and OH- as the main components, and the crystal system is hexagonal. In this study, we considered the application of the PC software "PyMOL" to hydroxyapatite. Although this software requires the three- dimensional coordinates of each molecule, we could use the data which were obtained in our previous study. Using this software, we can freely view the stereo structure of any molecules from any direction simply by operating a PC mouse. In addition to the CG of hydroxyapatite, we could show the CG of fluoridated hydroxyapatite with the partial substitution of OH^- by F^-, and Mg-containing hydroxyapatite with that of Ca^{2+} by Mg^{2+}.

Volume 1 Issue 6 November 2017

Introduction

Bone and teeth are composed of an inorganic hydroxyapatite and organic collagen. Tooth enamel contains more than 95% of highly crystallized hydroxyapatite, while bone and tooth dentine contain 60-70% of poorly crystallized hydroxyapatite [1,2]. Strictly speaking, they are carbonate-containing hydroxyapatites, so-called "carbonate apatites" (CO_3Ap), which contain several % of CO_3^{2-} ions [3].

Stoichiometric hydroxyapatite (HAp: $Ca_{10}(PO_4)_6(OH)_2$) is an ionic crystal with Ca^{2+}, PO_4^{3-}, and OH^- as the main components, and the crystal system is hexagonal (a = b = 9.432 Å, c = 6.881 Å, α = β = 90º, γ = 120º) [4,5]. It has been reported that almost all elements in the periodic table can adopt the positions of the main components above-mentioned [6]. Therefore, "apatites" has the meaning of thieves because they are very complicated substances from the Greek language. Thus, real apatites contain many trace elements.

The analysis of hydroxyapatite was delayed until 1964 [5], although the crystal structure of fluorapatite (FAp: $Ca_{10}(PO_4)_6F_2$) was initially analyzed in 1930 by Náray-Szabó [7]. Because OH^- ions in hydroxyapatite shift just 0.3 Å from the stable position, it was difficult to determine the accurate crystal structure solely by X-ray diffraction analysis. Finally, it was determined by combining with neutron diffraction analysis [8]. Hydroxyapatite is sudo-hexagonal (rhombohedral), while FAp is a typical hexagonal crystal. Due to the development of computer science, Okazaki and Sato [9] could successfully construct a crystal model of HAp with a personal computer and the program "PROTGRA" [10]. In their paper, the computer graphics (CG) of HAp and FAP were shown accurately according to the radii of Ca^{2+} (0.99 Å),

P^{5+} (0.33 Å), O^{2-} (1.40 Å), H^{+} (negligible), and F^{-} (1.36 Å) based on the data of Pauling [11]. OH^{-} ions in hydroxyapatite shift just 0.3 Å from the stable position, while F^{-} ions in fluorapatite are present at levels of just 1/4 and 3/4 of the height of the crystal unit cell. Lattice dimensions of a = 9.37 Å and c = 6.88 Å were adopted from the data reported by Náray-Szabó [7]. Compared with the structure of hydroxyapatite, that of fluorapatite can readily be seen to be crystallographically more stable. The computer graphics display demonstrated that fluoride ions serve to stabilize the hydroxyapatite crystals and prevent dental caries.

Methods

Recently, the PC software "PyMOL", which can draw polymer CG on Windows, is often used worldwide. We considered the application of "PyMOL" to hydroxyapatite. At present, "PyMOL" is licensedby Schrödinger. We have already succeeded in the CG drawing of tetrafluoroethylene (PTFE) [12]. Using this software, we can freely view the stereo structure of any molecules. However, this software requires the three- dimensional coordinates of each molecule. Fortunately, we could use the data shown in Table 1, which were obtained in our previous study [9].

HETATM	1	O	ALA 1	1	-3.019	2.673	5.161	1.00	0.00	O
HETATM	2	O	ALA 1	2	-1.697	5.496	1.720	1.00	0.00	O
HETATM	3	O	ALA 1	3	0.805	3.951	1.720	1.00	0.00	O
HETATM	4	O	ALA 1	4	-0.892	9.447	5.161	1.00	0.00	O
HETATM	5	O	ALA 1	5	0.892	6.890	1.720	1.00	0.00	O
HETATM	6	O	ALA 1	6	3.824	1.278	5.161	1.00	0.00	O
HETATM	7	O	ALA 1	7	5.608	-1.278	1.720	1.00	0.00	O
HETATM	8	O	ALA 1	8	3.911	4.217	5.161	1.00	0.00	O
HETATM	9	O	ALA 1	9	6.413	2.673	5.161	1.00	0.00	O
HETATM	10	O	ALA 1	10	7.735	5.496	1.720	1.00	0.00	O
HETATM	11	O	ALA 1	11	-3.097	3.350	1.720	1.00	0.00	O
HETATM	12	O	ALA 1	12	-1.619	4.819	5.161	1.00	0.00	O
HETATM	13	O	ALA 1	13	-0.266	9.176	1.720	1.00	0.00	O
HETATM	14	O	ALA 1	14	0.266	7.161	5.161	1.00	0.00	O
HETATM	15	O	ALA 1	15	1.353	4.357	5.161	1.00	0.00	O
HETATM	16	O	ALA 1	16	3.363	3.811	1.720	1.00	0.00	O
HETATM	17	O	ALA 1	17	4.450	1.007	1.720	1.00	0.00	O
HETATM	18	O	ALA 1	18	4.982	-1.007	5.161	1.00	0.00	O
HETATM	19	O	ALA 1	19	6.335	3.350	1.720	1.00	0.00	O
HETATM	20	O	ALA 1	20	7.813	4.819	5.161	1.00	0.00	O
HETATM	21	O	ALA 1	21	-3.899	5.345	0.506	1.00	0.00	O
HETATM	22	O	ALA 1	22	-3.899	5.345	2.934	1.00	0.00	O
HETATM	23	O	ALA 1	23	-0.817	2.824	3.947	1.00	0.00	O
HETATM	24	O	ALA 1	24	-0.817	2.824	6.375	1.00	0.00	O
HETATM	25	O	ALA 1	25	-1.862	7.464	3.947	1.00	0.00	O
HETATM	26	O	ALA 1	26	-1.862	7.464	6.375	1.00	0.00	O
HETATM	27	O	ALA 1	27	2.037	2.120	0.506	1.00	0.00	O
HETATM	28	O	ALA 1	28	2.037	2.120	2.934	1.00	0.00	O
HETATM	29	O	ALA 1	29	2.854	-0.704	3.947	1.00	0.00	O
HETATM	30	O	ALA 1	30	2.854	-0.704	6.375	1.00	0.00	O
HETATM	31	O	ALA 1	31	1.862	8.872	0.506	1.00	0.00	O
HETATM	32	O	ALA 1	32	1.862	8.872	2.934	1.00	0.00	O
HETATM	33	O	ALA 1	33	2.679	6.049	3.947	1.00	0.00	O
HETATM	34	O	ALA 1	34	2.679	6.049	6.375	1.00	0.00	O
HETATM	35	O	ALA 1	35	6.578	0.704	0.506	1.00	0.00	O
HETATM	36	O	ALA 1	36	6.578	0.704	2.934	1.00	0.00	O
HETATM	37	O	ALA 1	37	5.533	5.345	0.506	1.00	0.00	O
HETATM	38	O	ALA 1	38	5.533	5.345	2.934	1.00	0.00	O
HETATM	39	O	ALA 1	39	8.615	2.824	3.947	1.00	0.00	O
HETATM	40	O	ALA 1	40	8.615	2.824	6.375	1.00	0.00	O

HETATM	41	P	ALA 1	41	-3.114	4.902	1.720	1.00	0.00	P
HETATM	42	P	ALA 1	42	-1.602	3.267	5.161	1.00	0.00	P
HETATM	43	P	ALA 1	43	-1.086	7.922	5.161	1.00	0.00	P
HETATM	44	P	ALA 1	44	2.028	3.021	1.720	1.00	0.00	P
HETATM	45	P	ALA 1	45	3.630	-0.246	5.161	1.00	0.00	P
HETATM	46	P	ALA 1	46	1.086	8.414	1.720	1.00	0.00	P
HETATM	47	P	ALA 1	47	2.688	5.148	5.161	1.00	0.00	P
HETATM	48	P	ALA 1	48	5.802	0.246	1.720	1.00	0.00	P
HETATM	49	P	ALA 1	49	6.318	4.902	1.720	1.00	0.00	P
HETATM	50	P	ALA 1	50	7.830	3.267	5.161	1.00	0.00	P
HETATM	51	CA	ALA 1	51	0.000	5.445	0.000	1.00	0.00	CA
HETATM	52	CA	ALA 1	52	0.000	5.445	3.447	1.00	0.00	CA
HETATM	53	CA	ALA 1	53	0.000	5.445	6.888	1.00	0.00	CA
HETATM	54	CA	ALA 1	54	4.716	2.723	0.000	1.00	0.00	CA
HETATM	55	CA	ALA 1	55	4.716	2.723	3.447	1.00	0.00	CA
HETATM	56	CA	ALA 1	56	4.716	2.723	6.888	1.00	0.00	CA
HETATM	57	CA	ALA 1	57	-3.583	6.105	5.161	1.00	0.00	CA
HETATM	58	CA	ALA 1	58	-1.133	2.063	1.720	1.00	0.00	CA
HETATM	59	CA	ALA 1	59	-2.363	8.118	1.720	1.00	0.00	CA
HETATM	60	CA	ALA 1	60	1.221	2.013	5.161	1.00	0.00	CA
HETATM	61	CA	ALA 1	61	2.353	-0.051	1.720	1.00	0.00	CA
HETATM	62	CA	ALA 1	62	2.363	8.219	5.161	1.00	0.00	CA
HETATM	63	CA	ALA 1	63	3.495	6.156	1.720	1.00	0.00	CA
HETATM	64	CA	ALA 1	64	7.079	0.051	5.161	1.00	0.00	CA
HETATM	65	CA	ALA 1	65	5.849	6.105	5.161	1.00	0.00	CA
HETATM	66	CA	ALA 1	66	8.299	2.063	1.720	1.00	0.00	CA
HETATM	67	O	ALA 1	67	0.000	0.000	2.112	1.00	0.00	O
HETATM	68	O	ALA 1	68	9.432	0.000	2.112	1.00	0.00	O
HETATM	69	O	ALA 1	69	-4.716	8.168	2.112	1.00	0.00	O
HETATM	70	O	ALA 1	70	4.716	8.168	2.112	1.00	0.00	O
HETATM	71	O	ALA 1	71	0.000	0.000	5.553	1.00	0.00	O
HETATM	72	O	ALA 1	72	9.432	0.000	5.553	1.00	0.00	O
HETATM	73	O	ALA 1	73	-4.716	8.168	5.553	1.00	0.00	O
HETATM	74	O	ALA 1	74	4.716	8.168	5.553	1.00	0.00	O
HETATM	75	H	ALA 1	75	0.000	0.000	3.016	1.00	0.00	H
HETATM	76	H	ALA 1	76	9.432	0.000	3.016	1.00	0.00	H
HETATM	77	H	ALA 1	77	-4.716	8.168	3.016	1.00	0.00	H
HETATM	78	H	ALA 1	78	4.716	8.168	3.016	1.00	0.00	H
HETATM	79	H	ALA 1	79	0.000	0.000	6.456	1.00	0.00	H
HETATM	80	H	ALA 1	80	9.432	0.000	6.456	1.00	0.00	H
HETATM	81	H	ALA 1	81	-4.716	8.168	6.456	1.00	0.00	H
HETATM	82	H	ALA 1	82	4.716	8.168	6.456	1.00	0.00	H
END										

Table 1: *Three-dimensional coordinates (X, Y and Z) of each molecule of hydroxyapatite.*

The atomic radius of each element is set as the Von der Waals radius by default, and a ball and stick (BS) model is initially drawn. Therefore, each radius was changed into an ionic radius based on Pauling data [11], and then modified slightly to be able to visualize it clearly as follows: Ca^{2+} (0.99 Å), P^{5+} (0.33 Å → 0.70 Å), O^{2-} (1.40 Å → 1.20 Å), H^{+} (negligible → 0.40 Å), F^{-} (1.36 Å → 1.20 Å), and Mg^{2+} (0.65 Å)

Computer Graphics

Figure 1 shows the original BS model of the hydroxyapatite with the Van der Waals radius displayed from directions perpendicular (Figure 1A) and parallel (Figure 1B) to the c-axis. Figure 2 is an ionic model observed from the same direction as Figure 1. Figure 3 shows the posterior view. We can view the structure freely from any direction simply by operating a PC mouse.

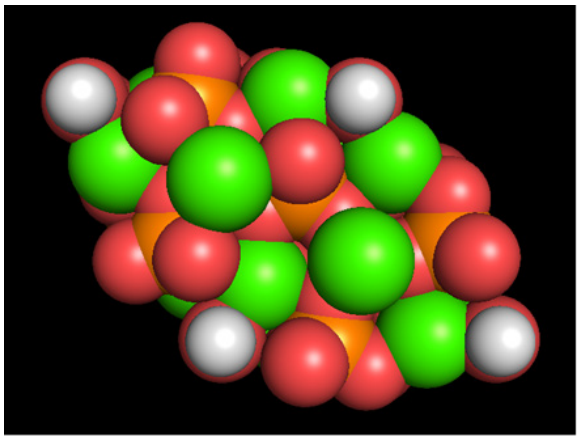

Figure 1: *Computer graphics-based Van der Waals model of hydroxyapatite viewed from directions perpendicular (A) and parallel (B) to the c-axis (A), with data obtained by Okazaki and Sato [9] using Windows.*

A B

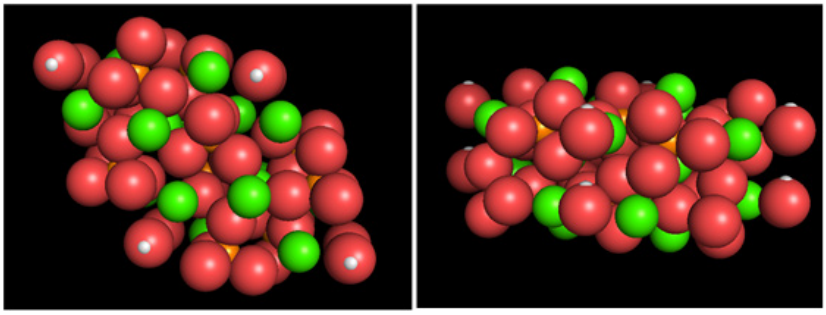

Figure 2: *Computer graphics-based ionic model of hydroxyapatite viewed from directions perpendicular (A) and parallel (B) to the c-axis (A). The ionic radii are changed rather than the value of Pauling [11]. Ca^{2+} (0.99 Å, green), P^{5+} (0.33 Å → 0.70 Å, orange), O^{2-} (1.40 Å → 1.20 Å, red), H^{+} (negligible → 0.40 Å, white).*

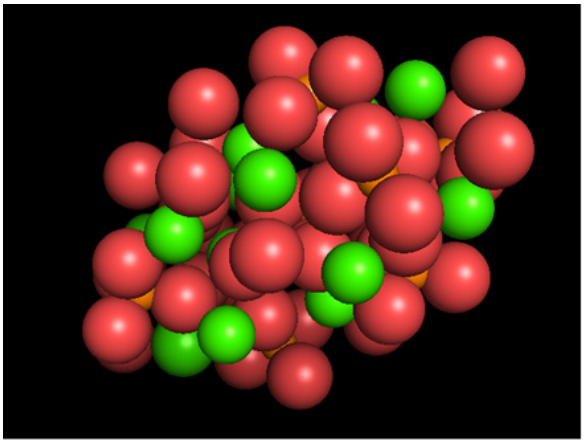

Figure 3: *Computer graphics-based ionic model of hydroxyapatite rotated to give a posterior view.*

Furthermore, as mentioned above, almost all of the elements in the periodic table can replace for the main components of Ca^{2+}, PO_4^{3-}, and OH^- [4]. Figure 4, as an example, shows the CG of fluoridated hydroxyapatite with the partial substitution of OH^- by F^- (Figure 4A), and Mg-containing hydroxyapatite with that of Ca^{2+} by Mg^{2+} (Figure 4B). Interestingly, some of the crystallographic properties of partially substituted fluoridated hydroxyapatites still remain unknown, although many studies have been conducted [13-16].

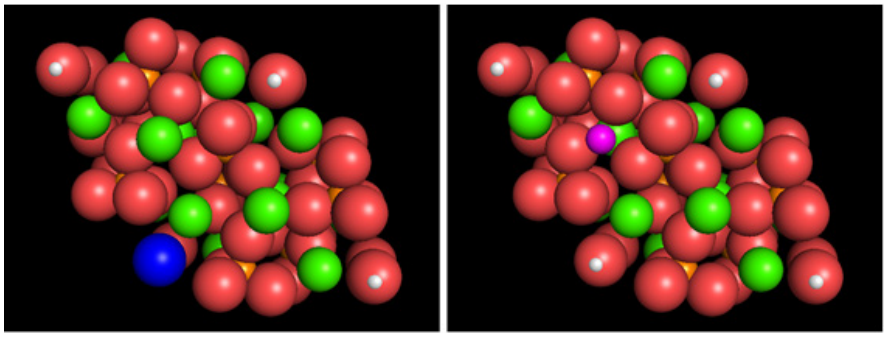

Figure 4: *The CG of fluoridated hydroxyapatite partially substituted by F^- for OH^- (A), and Mg-containing hydroxyapatite partially substituted by Mg^{2+} for Ca^{2+} (B). F^- (1.36 Å → 1.20 Å, blue), and Mg^{2+} (0.65 Å, purple)*

Future Trends

Bological apatites such as bone and teeth are carbonate-containing hydroxyapatite (CO_3Ap). A number of crystallographic studies on CO_3Ap have been reported [3,15, 17-20]. Enamel apatite contains 1~3 wt% of CO_3^{2-} ions, and bone and dentine contain more CO_3^{2-} ions, 5~6 wt% [2]. It is known that CO_3^{2-} ions of biological apatites, which are created in aqueous solution, adopt mainly PO_4^{3-} positions, contrary to CO_3Ap synthesized under dry conditions at a high temperature, in which CO_3^{2-} ions adopt OH^- positions. Interestingly, since the molecular weight of hydroxyapatite is 1,000 and that of CO_3^{2-} ions is 60 (6 wt%), in the case of bone apatite, approximately one CO_3^{2-} ion can replace six PO_4^{3-} ions in a unit cell of hydroxyapatite.

We can also draw the CG of CO_3Ap. However, the accurate direction of CO_3^{2-} is still unknown, because the content of CO_3^{2-} ions in CO_3Ap is small, and the crystallinity of CO_3Ap decreases with an increase in the CO_3^{2-} ion content. At present, we consider the possibility of CO_3^{2-} existing parallel to the c-axis being strong from the viewpoint of the shortening of the a-axis observed on X-ray diffraction analysis.

References

1. Brown WE. "Crystal growth of bone mineral". *Clinical Orthopaedics and Related Research* 44 (1966): 205-220.
2. Miles AEW. "Structural and Chemical Organization of Teeth. Vol. II". *New York, Academic Press* (1967).
3. LeGeros RZ. "Calcium Phosphates in Oral Biology and Medicine". *Basel, Karger* (1991).
4. Cullity BD. "Elements of X-Ray Diffraction. Second Ed". *Reading, Addison-Wesley Publishing Company* (1978).
5. Kay MI., *et al.* "Crystal structure of hydroxyapatite". *Nature* 204 (1964): 1050-1052.
6. Van Wazer JR. "Phosphorus and Its Compounds". *New York, Interscience* (1958).
7. St Náray-Szabó. "The structure of apatite $(CaF)Ca_4(PO_4)_3$". *Z Kristallogr* 75.1 (1930): 387.
8. Sudarsanan K and Young RA. "Significant precision in crystal structure details: Holly springs hydroxyapatite". *Acta Crystallographica Section* B25 (1969): 1534-1543.
9. Okazaki M and Sato M. "Computer graphics of hydroxyapatite and beta-tricalcium phosphate". *Biomaterials* 11.8 (1990): 573-578.
10. Nakano H. "Graphics display of protein by personal computer". *Information* 5.10 (1986): 65
11. Pauling L. "The Nature of the Chemical Bond. 3rd edn". Ithaca, Cornell University Press (1960).

12. Furuta M., *et al.* "Molecular level analyses of mechanical properties of PTFE sterilized by Co-60 γ-ray irradiation for clinical use". *Radiation Physics and Chemistry* 139 (2017): 126-131.
13. Moreno EC., *et al*. "Physicochemical aspects of fluoride apatite systems relevant to the study of dental caries". *Caries Research* 11 (Suppl. 1) (1977): 142-171.
14. Okazaki M., *et al*. "Solubility and crystallinity in relation to fluoride content of fluoridated hydroxyapatites". *Journal of Dental Research* 60 (1981): 845-849.
15. Elliott JC. "Structure and Chemistry of the Apatites and Other Calcium Orthophosphates". *Amsterdam, Elsevier* (1994).
16. Tohda H., *et al*. "Transmission electron microscopic observation of heterogeneous fluoridated hydroxyapatites". *Biomaterials* 16.12 (1995): 945-950.
17. LeGeros RZ., *et al.* "Apatite crystallites: Effects of carbonate on morphology". *Science* 155.3768 (1967): 1409-1411.
18. Okazaki M., *et al*. "Solubility behavior of CO_3 apatites in relation to crystallinity". *Caries Research* 15.6 (1981): 477-483.
19. Okazaki M., *et al.* "Insolubilized properties of UV-irradiated CO_3 apatite-collagen composites". *Biomaterials* 11.8 (1990): 568-572.
20. Yamasaki Y., *et al.* "Action of FGMgCO_3Ap-collagen composite in promoting bone formation". *Biomaterials* 24.27 (2003): 4913-4920.